



Phosphorylated nuclear factor erythroid 2-related factor 2 promotes the secretion of C-C motif chemokine ligand 2 and the recruitment of M2 macrophages

Zhanghao Huang^{1,2,3#}, Xing Li^{1,2,3#}, Tingting Zhou^{1,2,3#}, Yun Jiang⁴, Jia-Hai Shi^{2,3}

¹Medical College of Nantong University, Nantong, China; ²Nantong Key Laboratory of Translational Medicine in Cardiothoracic Diseases, and Research Institution of Translational Medicine in Cardiothoracic Diseases, Affiliated Hospital of Nantong University, Nantong, China; ³Department of Thoracic Surgery, Affiliated Hospital of Nantong University, Nantong, China; ⁴Department of Cardiothoracic Surgery, Affiliated Hospital of Nantong University, Nantong, China

Contributions: (I) Conception and design: Z Huang; (II) Administrative support: JH Shi, Y Jiang; (III) Provision of study materials or patients: X Li, T Zhou; (IV) Collection and assembly of data: Z Huang; (V) Data analysis and interpretation: Z Huang; (VI) Manuscript writing: All authors; (VII) Final approval of manuscript: All authors.

[#]These authors contributed equally to this work.

Correspondence to: Yun Jiang, Department of Cardiothoracic Surgery, Affiliated Hospital of Nantong University, Nantong 226001, China. Email: nanjingjn292@163.com; Jia-Hai Shi, Nantong Key Laboratory of Translational Medicine in Cardiothoracic Diseases, and Research Institution of Translational Medicine in Cardiothoracic Diseases, Affiliated Hospital of Nantong University, Nantong 226001, China. Email: sjh@ntu.edu.cn.

Background: Nuclear factor erythroid 2-related factor 2 (Nrf2) has been shown to ameliorate early ischemia-reperfusion (I/R) injury after activation by tertiary butylhydroquinone (TBHQ). However, despite macrophage-associated inflammation being a distinguishing feature of I/R injury, the precise roles and mechanisms of Nrf2 in macrophage-associated inflammation are still poorly understood.

Methods: I/R and hypoxia/reperfusion (H/R) models were constructed *in vivo* using rats and *in vitro* using the H9C2 rat cardiomyoblast cell line, respectively. The effects of TBHQ on myocardial damage under oxidative stress were assessed using apoptosis and cell cycle assays, as well as echocardiography. The Jaspard database was used to identify the C-C motif chemokine ligand 2 (Ccl2) gene promoter as a possible binding site for Nrf2. This interaction was validated by chromatin immunoprecipitation (ChIP) assays, enzyme-linked immunosorbent assay (ELISA), immunofluorescence staining, and western blot analysis. Transwell migration assays were used to examine the migration ability of the recruited macrophages.

Results: The Nrf2 activator, TBHQ, induced phosphorylation of Nrf2 and promoted the secretion of Ccl2 by myocardial microvascular endothelial cells. The secreted Ccl2 induced the chemotaxis of M2 macrophages into the injury site and triggered the secretion of anti-inflammatory factors including interleukin (IL)-10 and tumor growth factor (TGF)- β 1 by M2 macrophages, thereby reducing early myocardial ischemia reperfusion injury (MI/R).

Conclusions: Activation of Nrf2 alleviated oxidative stress during myocardial ischemia and reperfusion by inducing the secretion of anti-inflammatory factors.

Keywords: Nuclear factor erythroid 2-related factor 2 (Nrf2); phosphorylated nuclear factor erythroid 2-related factor 2 (P-Nrf2); C-C motif chemokine ligand 2 (Ccl2); M2 macrophage; tumor growth factor (TGF)- β 1; interleukin (IL)-10

Submitted Jun 07, 2021. Accepted for publication Oct 15, 2021.

doi: 10.21037/atm-21-2947

View this article at: <https://dx.doi.org/10.21037/atm-21-2947>

Introduction

The incidence of acute myocardial infarction (AMI) caused by myocardial ischemia-reperfusion injury (MIRI) continues to escalate worldwide. Despite the application of reperfusion therapy, there is still a 25% incidence of heart failure and a close to 10% mortality. The recovery of blood supply after a long period of ischemia can lead to MIRI, which is a complex pathophysiological process involving metabolic dysfunction and myocardial tissue destruction (1). The potential mechanisms of MIRI are complex and may involve oxidative stress, calcium overload, mitochondrial dysfunction, and aggregation of inflammatory cells (2-4).

Nuclear factor erythroid 2-related factor 2 (Nrf2) is a transcription factor containing a leucine zipper. Kelch-like ECH-associated protein 1 (Keap1) forms part of the Cullin 3-dependent E3 ubiquitin ligase complex that regulates the stability and accumulation of Nrf2. Under physiological conditions, Keap1 binds to Nrf2, leading to the proteasomal degradation of the Nrf2 protein. The cysteine residue at position 151 (C151) of Keap1 is a sensitive sensor for changes in oxygen partial pressure. Under oxidative stress, the levels of intracellular reactive oxygen species (ROS) increase and the conformation of Keap1 changes, causing Nrf2 to dissociate from Keap1. When phosphoinositide 3-kinase (PI3K), protein kinase C (PKC), c-Jun N-terminal kinase (JNK) and other pathway molecules are activated and phosphorylated, they enter the nucleus and bind to Keap1. The resultant complexes can then bind the antioxidant response elements (AREs) located in the promoter region of various genes and activate the transcription of antioxidant genes such as heme oxygenase 1 (HO-1), phase II detoxification enzymes, proteasomes, and others (5).

Tertiary butylhydroquinone (TBHQ) is an agonist of Nrf2. It is an aromatic organic compound with highly efficient antioxidant function. Oxidation of the molecule releases H[•] free radicals, which exerts an antioxidant effect. In addition, TBHQ causes activation of phase II enzymes and the Nrf2 signaling pathway, resulting in significant antioxidant activity in various cell types and tissues. The chemical structure of TBHQ allows it to rapidly diffuse from the plasma membrane to the cytoplasm, acting as a ROS scavenger and inducing the dissociation of the Keap1/Nrf2 complex (6,7).

Chemokines are small molecular proteins that play important roles in numerous physiological processes in the human body. They are mostly secreted by immune cells and glial cells and have chemotactic activity. The C-C

motif chemokine ligand 2 (Ccl2), also known as monocyte chemoattractant protein-1 (MCP-1), is a member of the CC subfamily (also known as the β subfamily) of chemokines. Ccl2 can exert chemoattractant activity on monocytes, giant cells, and T lymphocytes, and stimulate phagocytosis and the production of antibodies, thereby resisting invasion by foreign microorganisms.

While a moderate inflammatory response is a self-protective mechanism, a dysregulated inflammatory response can cause severe damage to the body. Under appropriate stimulation, macrophages are activated into an inflammatory state, which can be classified as M1 (classical activation) or M2 (alternative activation). M1 macrophages have pro-inflammatory effects related to the immune response to bacterial and intracellular pathogens, while M2 macrophages have more anti-inflammatory effects and have related functions in angiogenesis and wound healing. M2-like macrophages have regulatory activity, which are mainly identified based on the expression of CD209 (a C-type lectin) negatively regulating pro-inflammatory cytokines and inducing anti-inflammatory mediators such as interleukin (IL)-10 and tumor growth factor (TGF)- β 1. Both Nrf2 and macrophages play a pivotal role in myocardial ischemia and reperfusion; however, whether these macrophages are linked and the degree to which Ccl2 influences their interaction during myocardial ischemia and reperfusion remains to be fully elucidated. We present the following article in accordance with the ARRIVE reporting checklist (available at <https://dx.doi.org/10.21037/atm-21-2947>).

Methods

Cells and animals

The H9C2 rat cardiomyoblast cell line was obtained from the Cell Bank of the Chinese Academy of Sciences (Shanghai, China). The medium of H9C2 is Dulbecco's Modified Eagle Medium (DMEM), excluding supplement. Male Sprague Dawley rats (250 \pm 10 g, 8 weeks old) were purchased from the Model Animals Research Center of Nantong University (Nantong, China). Rats were housed in a specific pathogen-free (SPF) environment at 22 \pm 1 °C with a relative humidity of 50 \pm 1% and a normal 12-h day/night cycle. Rats were housed in the Nantong University in a pathogen-free environment with ad libitum access to food and water and were maintained under a 14-h light/10-h dark cycle. All animal experiments were approved by the Medical Ethics Committee of Nantong University and conducted in

accordance with the guidance of the Experimental Institute of Nantong University. The study was approved by the ethics board of the Affiliated Hospital of Nantong University (No. S20200314-012).

The in vitro hypoxia/reperfusion model and the in vivo ischemia/reperfusion rat model

For the *in vitro* experiments, H9C2 cells were cultured to 80% confluency in normal culture medium (DMEM with 10% FBS). Cells were then cultured in medium without serum and sugar at 37 °C for 4 h in a tri-atmosphere incubator under anoxia conditions consisting of 94% N₂, 5% CO₂ and 1% O₂. Cells were then cultured in normal medium under normoxic conditions to establish reoxidation. Cardiomyocytes that were not exposed to anoxia were considered the control group.

In vivo experiments were performed using 24 eight-week-old male Sprague Dawley rats. Rats were randomly allocated to the control group (n=6) or the treatment group (n=6). To induce I/R injury, rats were placed under general anesthesia, and the heart and the left anterior descending (LAD) artery were exposed at the fourth and intercostal space. A 6-0 silk thread was then used to ligate the LAD. After 30 min, this was removed to allow for reperfusion. The infarction was confirmed when the anterior wall of the left ventricle (LV) turned pale. TBHQ was administered intraperitoneally to different groups of rats (n=6) at concentrations of 0, 5, 10 and 20 mg/kg, with the order of injection being randomized. The vehicle for TBHQ administration was dimethyl sulfoxide (DMSO; Sigma-Aldrich, St. Louis, MO, USA). The solubility of TBHQ in DMSO was ≥ 56.66 mg/mL. A total of 0.2 mL DMSO was used to dissolve TBHQ of different concentrations, and 1.8 mL of physiological saline was used to dilute the TBHQ. The final injection volume of each experimental mouse was 2 mL. The control group was injected with 0.2 mL of DMSO plus 1.8 of mL saline (8-10).

Analysis of cell cytotoxicity and cell viability

To assess the cytotoxicity of TBHQ, H9C2 cells were inoculated in 96-well plates at a density of 5×10^3 cells/well, and incubated with different concentrations of TBHQ (0, 25, 50, 100, 200, 400 and 800 μ mol) for 24 h.

To assess the effects of TBHQ on cell viability, H9C2 cells were inoculated in 96-well plates and incubated for 24 h, which was followed by 4 h of hypoxia and 2 h

of reoxygenation. Cells were incubated with different concentrations of TBHQ during reoxygenation.

Cells were then washed with phosphate-buffered saline (PBS) and incubated with 3-(4, 5-dimethylthiazol-2-yl)-2, 5-diphenyltetrazolium bromide (MTT; Sigma-Aldrich) for 4 h (11). After addition of DMSO to each well, the absorbance was measured at 570 nm, and an automatic detection spectrophotometer (Bio-Rad; Richmond, CA, USA) was used to determine cell viability.

Determination of oxidative stress indicators

H9C2 cells and the supernatants were collected. The levels of lactate dehydrogenase (LDH), superoxide dismutase (SOD), malondialdehyde (MDA), and glutathione peroxidase (GPX) were measured using a commercial kit (Beyotime, Shanghai, China) as described previously (12-14). The intensity was observed using a microplate reader.

To determine intracellular ROS levels (Beyotime), 1×10^4 H9C2 cells were incubated with and 2',7'-dichlorofluorescein diacetate (DCFH-DA) at 37 °C for 20 min. Flow cytometry (Attune NxT, Invitrogen, Waltham, MA, USA) analysis was performed to detect the average intracellular fluorescence intensity and the level of ROS.

Analysis of cell apoptosis and the cell cycle

Following hypoxia and reperfusion treatment, H9C2 cells were digested with trypsin-EDTA. After the digestion was terminated, cells were resuspended in 1 \times binding buffer and incubated at 37 °C for 10 min. Propidium iodide (PI) and Annexin V (Meilunbio[®], Shanghai, China) were added to the cell suspension. During this period, the control cells of the 3 groups were placed in a water bath at 52 °C for 2 min and 30 s, and then each group of cells was resuspended with 100 μ L of 1 \times binding buffer. The control cells of the 3 groups were stained with PI, Annexin V, or PI + Annexin V. Cells were then incubated in the dark for 15 min. One sample of cells without any dye was used as a blank control.

To assess the cell cycle, H9C2 cells were resuspended in 50 μ L of PBS and 950 μ L of 70% precooled alcohol. Samples were vortexed and immediately stored at -20 °C overnight. Cells were washed twice with precooled PBS and stained with PI solution (0.05 mg/mL of PI and 1 mg/mL of RNase A; Sigma-Aldrich). After being incubated for 30 min in the dark, all samples were assessed using flow cytometry (Attune NxT, Invitrogen) and the AttuneTM NxT software

(v2.7.0) as previously described (15,16).

Determination of cardiac function via echocardiography

To determine cardiac function, transthoracic echocardiograms were performed on rats using echocardiography, as described previously (17). Under sedation with chloral hydrate (300 mg/kg administered intraperitoneally), rats were placed in a supine position on a heating pad, and 2-dimensional and M-mode echocardiography was used to assess wall motion, chamber dimensions, and cardiac function (18).

Chromatin immunoprecipitation (ChIP) assay and enzyme-linked immunosorbent assay (ELISA) analysis

The Nrf2 binding site on the rat Ccl2 gene promoter was predicted using the Jasp database. ChIP analysis was performed using the EZ-ChIP Assay kit, according to the manufacturer's instructions [17-371, Millipore-Upstate, Temecula, CA, USA] (19). The H9C2 cells were cross-linked by adding 1% formaldehyde to the medium. Using the Branson Digital Sonifier (Type 450 with micro-tip probe), the DNA was cut into 200–1,000 bp fragments by 12 ultrasonic treatments at 10- and 60-s pulse intervals. The isotype immunoglobulin G (IgG) was used as a negative control. The cross-linked DNA samples were reversed by Proteinase K, and ChIP-enriched DNA samples were obtained, with a spin column being used for purification. Precipitated DNA was analyzed by real-time polymerase chain reaction (PCR) using the following Ccl2 promoter primers: forward 5'-CGCAGCTTCATTTGCTCCCA and reverse 5'-CAGAGGGTGGAGTCAGGCAG. The resulting product was separated by 1% agarose gel electrophoresis. The collected cell supernatant was used to evaluate the concentration of Ccl2 in the supernatant by ELISA (Elabscience Biotechnology Co. Ltd, Wuhan, China), according to manufacturer's instructions.

Immunohistochemistry and immunofluorescence analysis

Rat hearts were excised and fixed with 4% paraformaldehyde for 24 h. For immunohistochemistry, the heart was embedded in paraffin, and 4- μ m sections were prepared. The sections were incubated with the retrieval repair solution in a water bath for 30 min after deparaffinization, followed by blocking of endogenous peroxidase with 3% H₂O₂ for 15 min. After incubation with goat serum for 2 h,

sections were treated with a rabbit anti-CD68 antibody (1:200, Proteintech, Chicago, IL, USA) at 4 °C overnight. Finally, the sections were stained with 3,3'-diaminobenzidine (DAB; Sigma-Aldrich).

For immunofluorescence analysis, the heart was dehydrated with gradient sucrose (10%, 20% and 30%). The samples were frozen and cut into 12- μ m slices and dried for 24 h. Samples were incubated with primary antibody overnight at 4 °C, such as anti-Ccl2 antibody (1:200, EMD Millipore, Temecula, CA, USA), anti-CD206 antibody (1:200, Proteintech), anti-iNOS antibody (1:200, Proteintech), anti-CD14 antibody (1:200, Proteintech), and anti-CD11b antibody (1:200, ABclonal Technology Co.,Ltd, Wuhan, China). After being washed 3 times with PBS, the slices were stained with DAPI (4',6-diamidino-2-phenylindole, Sigma-Aldrich) and analyzed with a fluorescence microscope (Leica DMR 3000; Leica, Bensheim, Germany) to detect fluorescein isothiocyanate (FITC)-positive signals.

Extraction of primary macrophages

Rats were sacrificed and disinfected, which was followed by intraperitoneal administration of 15 mL of DMEM supplemented with antibiotics. After aspiration of the peritoneal exudate containing DMEM, the exudate was centrifuged at 1,000 rpm for 5 min and the pellet was resuspended. After 4 h, the supernatant was discarded and DMEM to was added to the primary macrophages.

Western blot analysis

The radioimmunoprecipitation assay (RIPA) solution was mixed with phenylmethylsulfonyl fluoride (PMSF; 1:100; Promega, Madison, WI, USA) and used for tissue homogenization. Samples were then centrifuged at 12,000 rpm at 4 °C for 20 min, and the supernatant was collected. The samples were loaded onto a 10% sodium dodecyl sulfate (SDS) polyacrylamide gel for electrophoresis and transferred to a polyvinylidene fluoride film. The membranes were blocked in 5% nonfat milk for 2 h at room temperature and then incubated overnight with primary antibodies, such as anti-Nrf2 antibody (1:1,000, Abcepta Biotech Ltd. Co. Suzhou, China), anti-P-Nrf2 antibody (1:1,000, Affinity Bioscience, Inc., Las Vegas, NV, USA), anti-Socs3 (1:1,000, Proteintech), anti-IL-10 antibody (1:1,000, Proteintech), anti-Tgf- β 1 antibody (1:1,000, Proteintech), anti- β -actin antibody (1:10,000, Proteintech),

and anti-Ccl2 antibody (1:1,000, EMD Millipore). Membranes were washed 3 times with Tris-buffered saline with Tween20 (TBST) for 10 min each time, followed by incubation with a IRDye800 conjugated secondary anti-rabbit antibody or mouse IgG (1:10,000, Rockland Gilbertsville, CA, USA) at room temperature for 2 h. Protein bands were visualized using the Odyssey Infrared Imaging System (LI-COR Biological Sciences, Lincoln, NE, USA), and optical density analyses were performed. All experiments were carried out at least three times.

Statistical analysis

Results are expressed as mean \pm standard deviation (SD). The parameter differences between two groups were analyzed using 1-way analysis of variance (ANOVA), and pairwise multiple comparisons were assessed using the Tukey test. All statistical analyses were conducted using the Prism software (GraphPad Software, San Diego, CA, USA). A P value <0.05 was considered statistically significant.

Results

TBHQ combats oxidative stress by activating Nrf2

The antioxidant response mediated by Nrf2 is helpful to improve the viability of H9C2 cells under oxidative stress damage. As an activator of Nrf2, TBHQ can induce cytoprotective genes. In many different models, the activation of Nrf2 can modulate immune responses. Normally cultured H9C2 cells were treated with gradient TBHQ (0, 25, 50, 100, 200, 400 and 800 μmol), and the cell viability of H9C2 was tested by MTT. When the TBHQ concentration was 50, 100 and 200 μmol , the cell viability was the same as the cells without TBHQ treatment. When the concentration of TBHQ were 25 μmol and greater than 200 μmol , TBHQ had a certain killing effect on H9C2 cells (*Figure 1A*) (20). After hypoxia and reoxygenation, H9C2 cells were treated with gradient TBHQ, and the activity of H9C2 cells was the highest when the concentration of TBHQ was 100 μmol (*Figure 1B*) (21). Through a comprehensive comparison, this study found that the best concentration of TBHQ was 100 μmol . After H9C2 cells underwent hypoxia and reoxygenation, the oxidative stress could be reflected by indicators such as ROS, LDH, MDA, SOD and GPX. Moreover, after 100 μmol TBHQ was added, Nrf2 was activated to reduce the damage caused by oxidative stress in the myocardium (*Figure 1C-1G*) (22).

TBHQ promotes phosphorylation of Nrf2 and reduces myocardial damage

Studies have proved that Nrf2 phosphorylation is the basis of Nrf2 activation. This study found that the expression of Nrf2 and phosphorylated Nrf2 (P-Nrf2) in H9C2 cells supplemented with 100 μmol TBHQ increased (*Figure 2A-2C*). Therefore, as an activator of Nrf2, TBHQ contributed to phosphorylating Nrf2 to P-Nrf2. After H9C2 hypoxia and reoxygenation, the normal oxidation/reduction dynamic balance was destroyed and a severe oxidative stress state was formed to induce cell apoptosis. Compared with H9C2 cells that without being treated by TBHQ, the expression of Nrf2 in H9C2 cells increased after 100 μmol TBHQ was added. The occurrence of Nrf2 in H9C2 cells could resist oxidative stress and significantly reduced the apoptosis rate (*Figure 2D-2F*) (23,24). Phosphorylation and dephosphorylation are the keys to control the cell cycle. The interphase of the cell cycle is divided into three phases, namely the early DNA synthesis period (G1), the DNA synthesis period (S), and the late DNA synthesis period (G2), which can be used as indicators to reflect cell proliferation. By comparing H9C2 after only hypoxia and reoxygenation, H9C2 cells supplemented with 100 μmol TBHQ accounted for a higher proportion in S phase, while the proportion of cells in G1 and G2 phases decreased (*Figure 2G-2K*) (25,26). The cardiac function of rats with gradient TBHQ (5, 10 and 20 mg/kg) intraperitoneal injection was significantly improved compared with rats not injected with TBHQ (*Figure 3A-3F*). The heart function of rats recovered best when the intraperitoneal injection of TBHQ reached 20 mg/kg, indicating that the functional recovery was promoted by P-Nrf2 (27,28).

Ccl2 transcription initiated by P-Nrf2

According to the former studies, as an important transcription factor in oxidative stress, Nrf2 can activate the transcription of the target gene by binding to the promoting region of the gene of interest. To figure out whether Nrf2 promotes transcription of Ccl2 by this method, this study predicted that the possible binding site of Nrf2 and Ccl2 promoters by using the Jaspar database and found that *Nrf2* and *Ccl2* gene bind in the promoter region (*Figure 4A*). The Schematic diagram of the binding site of Nrf2 on the rat Ccl2 promoter was shown in *Figure 4B*. Compared with H9C2 cells not injected with TBHQ, the expression of Ccl2

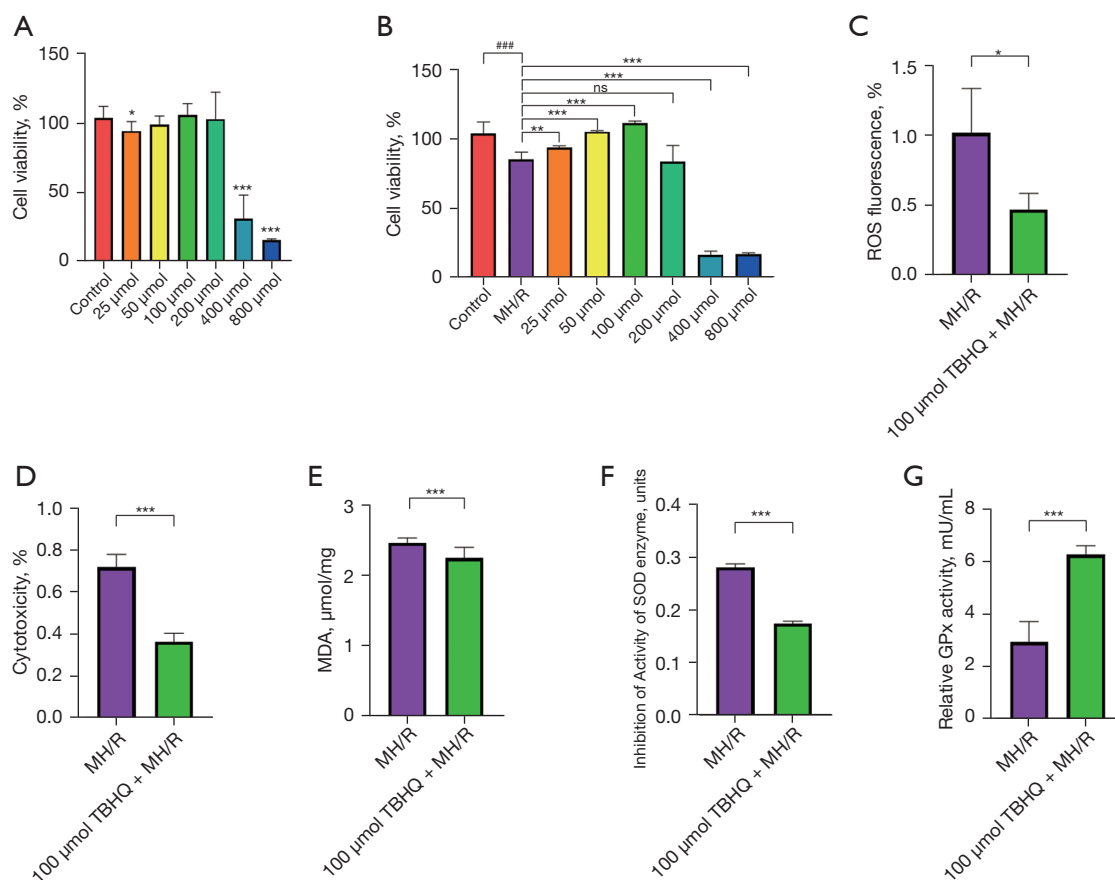


Figure 1 TBHQ enhanced the viability of cardiomyocytes via activation of Nrf2. (A) MTT assay showing the cytotoxicity caused by different concentrations of TBHQ in H9C2 cells. *, $P=0.0222$; ***, $P<0.0001$; 1-way ANOVA analysis, $n=9$, independent biological replicates. (B) MTT test showing the cytotoxicity of different concentrations of TBHQ on H9C2 cells after hypoxia and reoxygenation. ###, $P<0.001$; **, $P=0.0003$; ***, $P<0.0001$; 1-way ANOVA analysis, $n=9$, independent biological replicates. (C-G) The effects of TBHQ on the expression of ROS, LDH, MDA, SOD and GPX after hypoxia and reoxygenation. (C) *, $P=0.0176$; $n=4$. (D) ***, $P<0.0001$; $n=5$. (E) ***, $P<0.0001$; $n=10$. (F) ***, $P<0.0001$; $n=5$. (G) ***, $P<0.0001$; $n=7$. MH/R, myocardial hypoxia reperfusion; TBHQ, tertiary butylhydroquinone; Nrf2, nuclear factor erythroid 2-related factor 2; ANOVA, analysis of variance; ROS, reactive oxygen species; LDH, lactate dehydrogenase; MDA, malondialdehyde; SOD, superoxide dismutase; GPX, glutathione peroxidase.

in H9C2 cells injected with TBHQ was significantly increased (Figure 4C,4D). To further detect the secretion of Ccl2, the supernatant extracted from the cellular hypoxia/reperfusion (H/R) model was determined by the ELISA assay (29). The protein content of Ccl2 in cell secretions increased statistically, indicating that Nrf2 can promote the secretion of Ccl2 by initiating transcription (Figure 4E). ChIP analysis was conducted (30). The DNA fragments that may be bound by the Nrf2 antibody were first pulled down, and parallel qPCR detection was made to amplify the 190 bp fragment containing the predicted binding site. The results confirm that H/R can cause the binding of the transcription factor Nrf2 to the

promoter region of the Ccl2 gene to initiate the transcription of Ccl2 (Figure 4F). Immunofluorescence showed that the fluorescence intensity of Ccl2 in rats injected with 20 mg/kg TBHQ intraperitoneally was significantly higher than that in rats without TBHQ injection for 24 h after cardiac ischemia and reperfusion (31), which indicated that P-Nrf2 did cause the transcription of Ccl2 (Figure 4G,4H).

Nrf2 participates in macrophage recruitment by promoting Ccl2 secretion

The expression of CD68 in continuous sections was

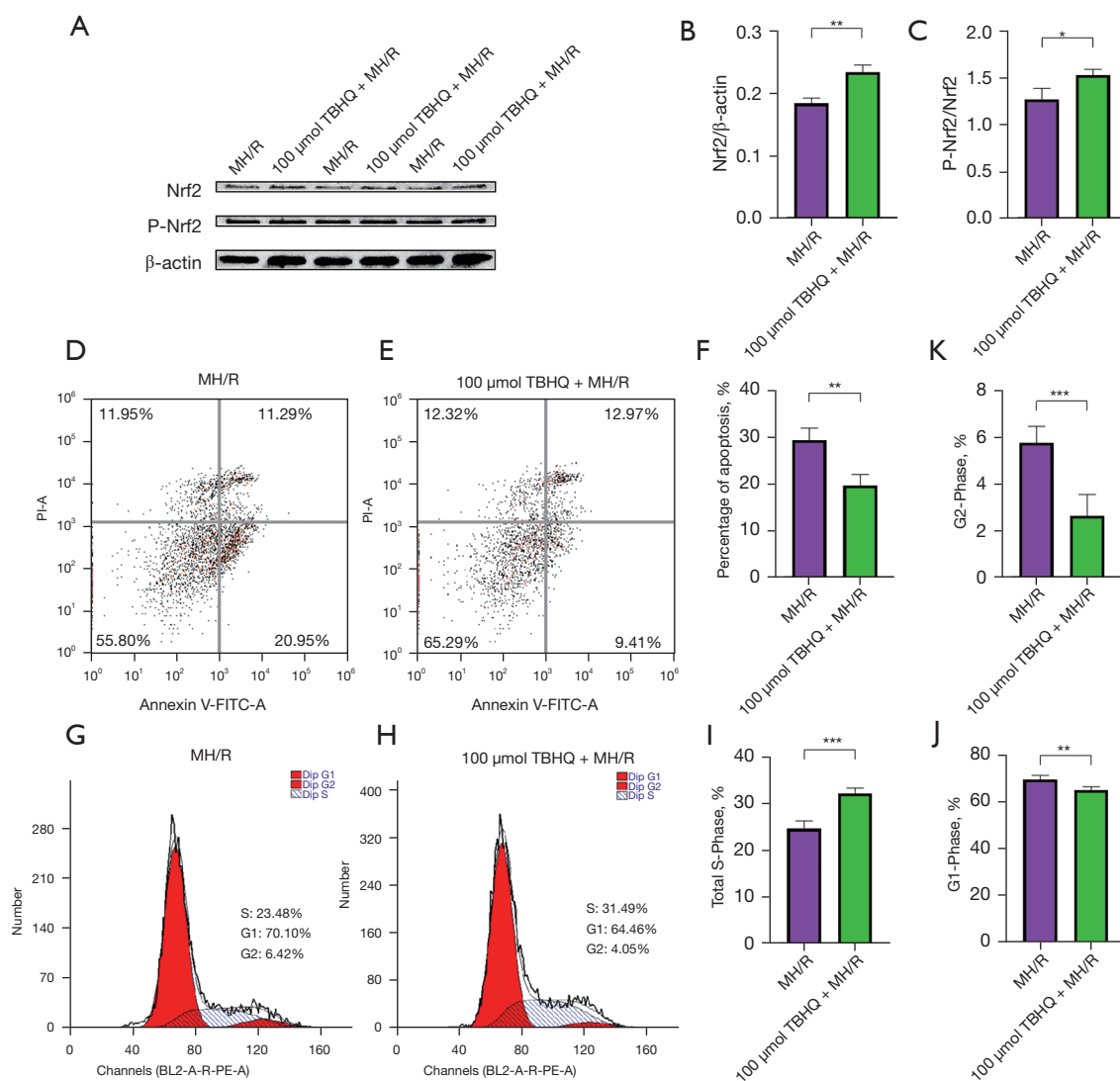


Figure 2 Phosphorylated Nrf2 reduced apoptosis. (A-C) Western blot analysis showing the protein expression of Nrf2 and P-Nrf2 in TBHQ-treated cells following hypoxia and reoxygenation. **, $P=0.0041$; *, $P=0.0256$; $n=3$. (D-F) Flow cytometry showing the effects of TBHQ on the apoptosis of H9C2 cells after hypoxia and reoxygenation. **, $P=0.0085$; $n=3$. (G-K) Flow cytometry displaying the influence of TBHQ on the cell cycle of H9C2 cells after hypoxia and reoxygenation. ***, $P<0.0001$; **, $P=0.0011$; $n=6$. MH/R, myocardial hypoxia reperfusion; Nrf2, nuclear factor erythroid 2-related factor 2; P-Nrf2, phosphorylated Nrf2; TBHQ, tertiary butylhydroquinone.

detected by immunohistochemistry. Compared with the normal heart (Figure 5A-5D) (32), CD68 were enriched in the infarction area. The H9C2 cells planted on the bottom of the 24-well plate were hypoxia for 4 and 2 h after reoxygenation (TBHQ was added during reoxygenation and removed after reoxygenation), the macrophages planted in the chamber were co-cultured with H9C2 cells 48 h (Figure 5E). After adding 4% paraformaldehyde to fix for 30 min, crystal violet staining for 20 min. Through

an observation of the bottom of the chamber under a microscope, the addition of TBHQ would increase the migration ability of macrophages. This result further confirmed that P-Nrf2 could promote the secretion of Ccl2, which in turn lead to the recruitment of macrophages (Figure 5F-5H). Immunofluorescence showed that the fluorescence intensity of CD14 (Figure 6A,6B) and CD11b (Figure 6C,6D) in rats injected with 20 mg/kg TBHQ intraperitoneally was higher than that in rats without TBHQ

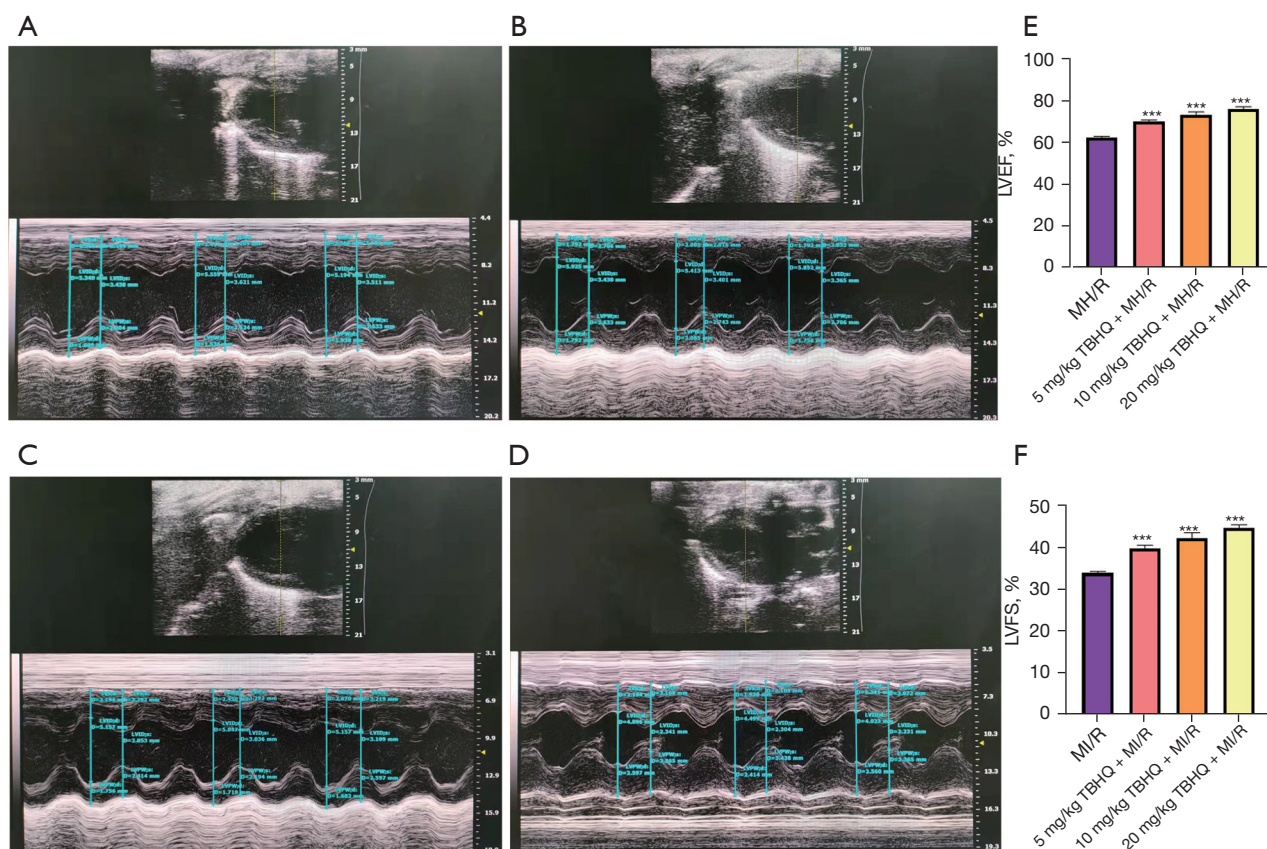


Figure 3 The effects of TBHQ on cardiac function. (A-D) Different concentrations of TBHQ (0, 5, 10, and 20 mg/kg) were injected intraperitoneally into rats, and echocardiography was performed to assess changes in cardiac function following ischemia-reperfusion injury. (E,F) The histogram shows the changes in LVEF and LVFS caused by different concentrations of TBHQ. (E) ***, (left to right) $P < 0.0001$, $P = 0.0003$, $P < 0.0001$. (F) ***, (left to right) $P = 0.0004$, $P = 0.0004$, $P < 0.0001$; $n = 3$. MI/R, myocardial ischemia reperfusion; TBHQ, tertiary butylhydroquinone; LVEF, left ventricular ejection fraction; LVFS, left ventricular fractional shortening.

injection for 24 h after cardiac ischemia and reperfusion, which indicated that Ccl2 did strengthen the recruitment of macrophages. The fluorescence intensity of iNOS (M1 macrophage marker) in rats injected with 20 mg/kg TBHQ intraperitoneally was slightly lower than in rats without TBHQ injection for 24 h after cardiac ischemia and reperfusion (Figure 6E,6F), while the fluorescence intensity of CD206 (M2 macrophage marker) in rats injected with 20 mg/kg TBHQ intraperitoneally was slightly higher than in rats without TBHQ injection for 24 h after cardiac ischemia and reperfusion (Figure 6G,6H).

Inflammatory factors are released by recruited M2 macrophages

The above experiments have proved that after H9C2 cells

undergo hypoxia and reoxygenation, after adding TBHQ, an activator of Nrf2, phosphorylation of Nrf2 caused the secretion of Ccl2, which in turn recruited macrophages. Meanwhile, this study extracted myocardial protein from I/R rats, and the expression of Nrf2, P-Nrf2, and Ccl2 was increased in the myocardium of rats intraperitoneally injected with 20 mg/kg TBHQ as verified by western blot analysis. The expression of SocS3 (M2 macrophage marker) in the myocardium of rats injected with TBHQ intraperitoneally was also increased (33), which implies that the macrophages recruited by secreted Ccl2 are mainly M2 type (34). Moreover, the expression of inflammatory factors such as Tgf- β 1 (35) and IL-10 (36) in the myocardium of rats injected with TBHQ intraperitoneally also increased, which verifies the former experimental results (Figure 7A-7G). In short, after myocardial ischemia-

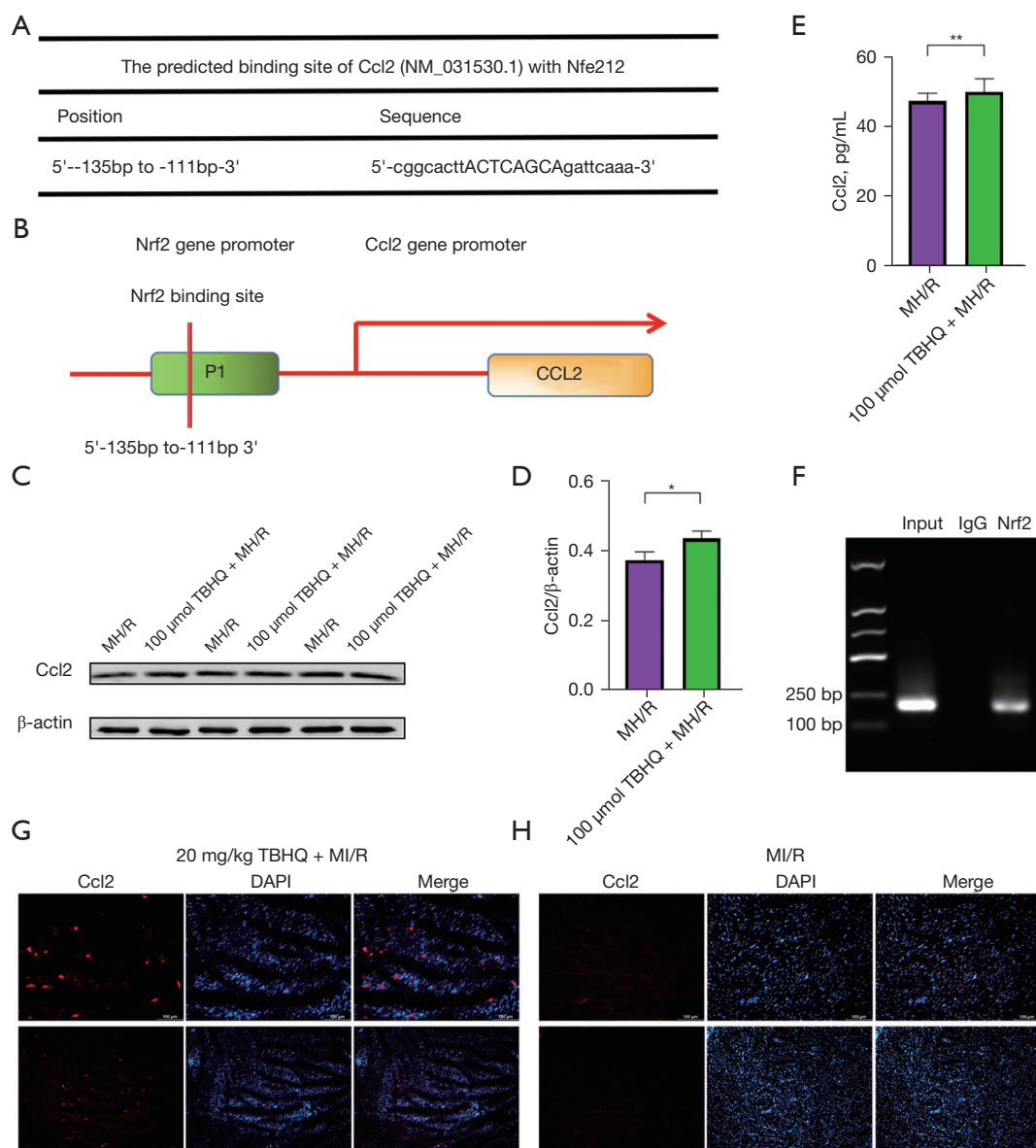


Figure 4 phosphorylated Nrf2 caused the secretion of Ccl2. (A,B) The Jasp database was used to predict the possible binding sites of Nrf2 with the Ccl2 promoters. (C,D) Western blot analysis showing the protein expression of Ccl2 in cells treated with TBHQ. *, $P=0.0298$; $n=3$. (E) ELISA showing that the activation of Nrf2 by TBHQ increased the secretion of Ccl2. **, $P=0.0057$; $n=24$. (F) ChIP analysis showing the effect of TBHQ on Ccl2 secretion. (G) Immunofluorescence staining showed the secretion of Ccl2 in rats administered 20 mg/kg TBHQ intraperitoneally. (H) Immunofluorescence showing the absence of Ccl2 secretion in rats that did not receive TBHQ injection. Nrf2, nuclear factor erythroid 2-related factor 2; Ccl2, C-C motif chemokine ligand 2; MH/R, myocardial hypoxia reperfusion; TBHQ, tertiary butylhydroquinone; ELISA, enzyme-linked immunosorbent assay; ChIP, Chromatin immunoprecipitation.

reperfusion, TBHQ can promote phosphorylation of Nrf2 and the secretion of transcription factor Ccl2, which in turn induces the recruitment of M2 macrophages and releases inflammatory factors, thereby reducing MIRI (Figure 8).

Discussion

The high rates of mortality in AMI can be largely attributed to inflammatory damage of myocardial cells due to ischemia-reperfusion injury. Under normal

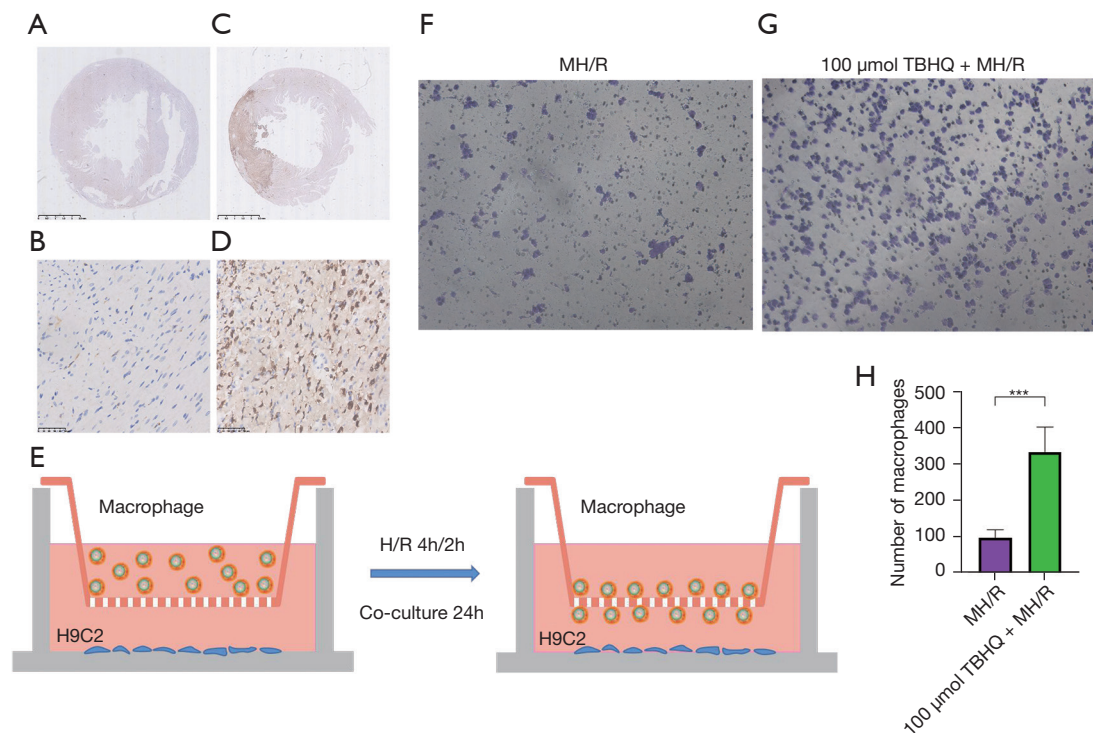


Figure 5 Secretion of Ccl2 caused the recruitment of macrophages. Immunohistochemical analysis showing the infiltration of macrophages in normal tissues (A,B) and ischemia-reperfusion tissues (C,D), staining method: immunohistochemistry; magnification: $\times 100$. After hypoxia and reoxygenation, H9C2 cells were co-cultured with primary cultured macrophages for 24 h, and the number of migrated macrophages was observed under a microscope. The migrated macrophages were stained by crystal violet staining (E-H), magnification: $\times 100$ (E,G). ***, $P < 0.0001$; $n = 6$. H/R, hypoxia/reperfusion; MH/R, myocardial hypoxia reperfusion; TBHQ, tertiary butylhydroquinone; Ccl2, C-C motif chemokine ligand 2.

circumstances, inflammation forms part of the host's active defense mechanism, but under pathological conditions, the prolongation or imbalance of inflammation can be associated with the pathogenesis of many diseases, such as cardiovascular disease and atherosclerosis.

During myocardial ischemia and reperfusion, the production of Nrf2 is protective against the damage caused by oxidative stress, which in itself is a self-defense mechanism of the myocardium (37,38). However, this mechanism provides minimal protection against the comparatively massive damage caused by oxidative stress. This study examined whether a moderate increase in the levels of Nrf2 can effectively improve myocardial injury.

Studies have shown that Nrf2 can be activated by two main mechanisms, which may have synergistic effects. This first involves the phosphorylation of Nrf2 via protein kinases such as PKC and PI3K. The second method involves the redox modification of the cysteine residue of the Keap1 protein. TBHQ is an activator of Nrf2 that

causes its phosphorylation. Phosphorylation of Nrf2 at Ser-40 by PKC is a key signaling event that can lead to ARE-mediated cellular antioxidant responses (39). Recent studies have suggested a role for Ccl2 as a macrophage chemoattractant and facilitator of tissue repair. Epidermal Nrf2 can activate the Nrf2/Ccl2/epidermal growth factor (EGF) signaling axis, resulting in a regeneration response through keratinocytes and promoting macrophage transport and re-epithelialization (40). When the Ccl2 chemokine interacts with the CCR2 chemokine receptor, the anti-inflammatory properties of intracellular signal transduction are initiated, suggesting that Ccl2 plays a role in the polarization of macrophages to obtain the M2 spectrum (41) and contributes to the re-epithelialization of wounds. Since the EGFR/MAPK signaling pathway can activate Nrf2, the Nrf2/Ccl2/EGF signaling axis may represent a potential positive regenerative feedback loop.

After reperfusion, M1 macrophages create a pro-inflammatory environment and remove cell debris, and

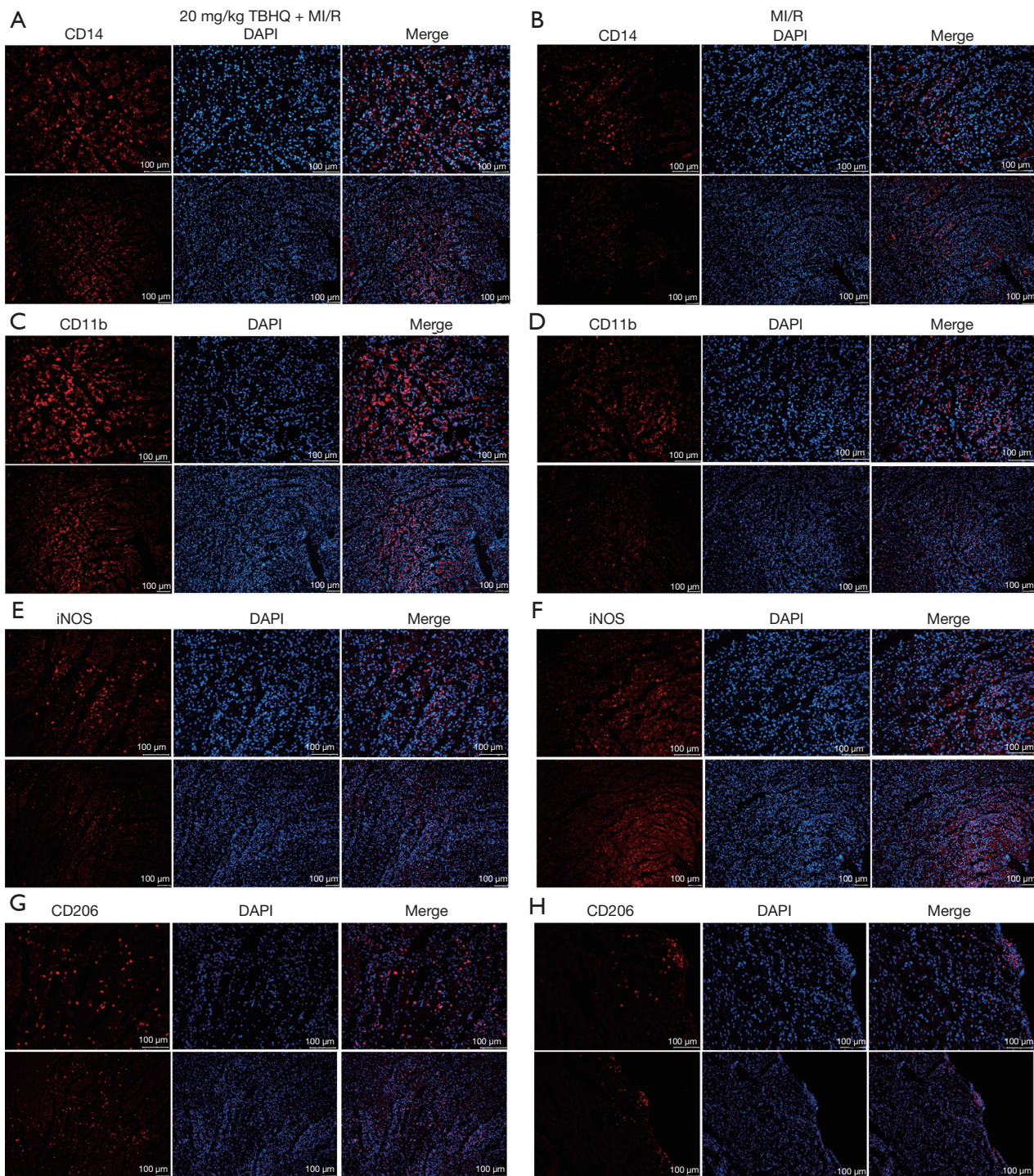


Figure 6 The recruited macrophages are polarized toward M2 type macrophages. Immunofluorescence showing the infiltration of macrophages in rats administered 20 mg/kg TBHQ intraperitoneally (A,C) and rats that did not receive TBHQ injection (B,D). (A,B) CD14. (C,D) CD11b. Immunofluorescence showing the infiltration of iNOS (M1 macrophages marker) in rats administered 20 mg/kg TBHQ intraperitoneally (E) and rats that did not receive TBHQ injection (F). Immunofluorescence showing the infiltration of CD206 (M2 macrophages marker) in rats administered 20 mg/kg TBHQ intraperitoneally (G) and rats that did not receive TBHQ injection (H). TBHQ, tertiary butylhydroquinone; MI/R, myocardial ischemia reperfusion.

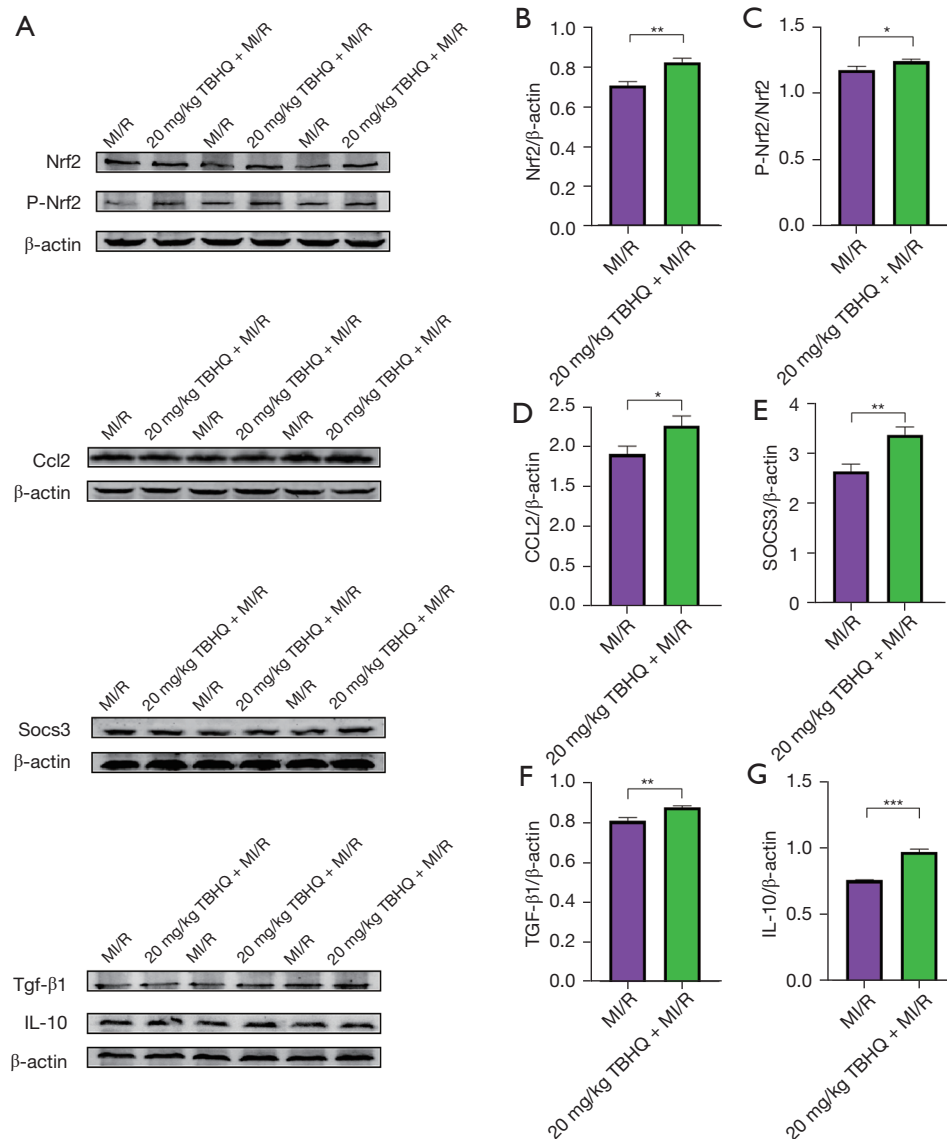


Figure 7 The recruited M2 type macrophages released inflammatory factors IL-10 and Tgf-β1. (A) Western blot showing an increase in the expression of Nrf2, P-Nrf2, Ccl2, SOCS3, IL-10 and TGF-β1 in rats injected with 20 mg/kg TBHQ intraperitoneally. (B-G) Histograms showing the expression of Nrf2, P-Nrf2, Ccl2, CD206, IL-10 and TGF-β in normal tissue and ischemia-reperfusion tissue. (B) **, P=0.0025. (C) *, P=0.027. (D) *, P=0.0179. (E) **, P=0.005. (F) **, P=0.0039. (G) ***, P<0.0001; n=3. MI/R, myocardial ischemia reperfusion; TBHQ, tertiary butylhydroquinone; Nrf2, nuclear factor erythroid 2-related factor 2; P-Nrf2, phosphorylated Nrf2; Ccl2, C-C motif chemokine ligand 2; SOCS3, suppressor of cytokine signaling 3; IL, interleukin; TGF, tumor growth factor.

gradually, M2 macrophages become more abundant. M2 macrophages not only secrete anti-inflammatory cytokines, but can also secrete a variety of growth factors, which play key roles in wound healing and scar formation. IL-10 is the most important cytokine with anti-inflammatory properties. It is produced by activated immune cells,

especially monocytes/macrophages and T cell subsets, and regulates the functions of many different immune cells (42). TGF-β1 is a multifunctional growth factor involved in regulating many developmental and physiological processes. Of particular importance is its role as an anti-inflammatory cytokine, and in this capacity, is able to inhibit or reverse

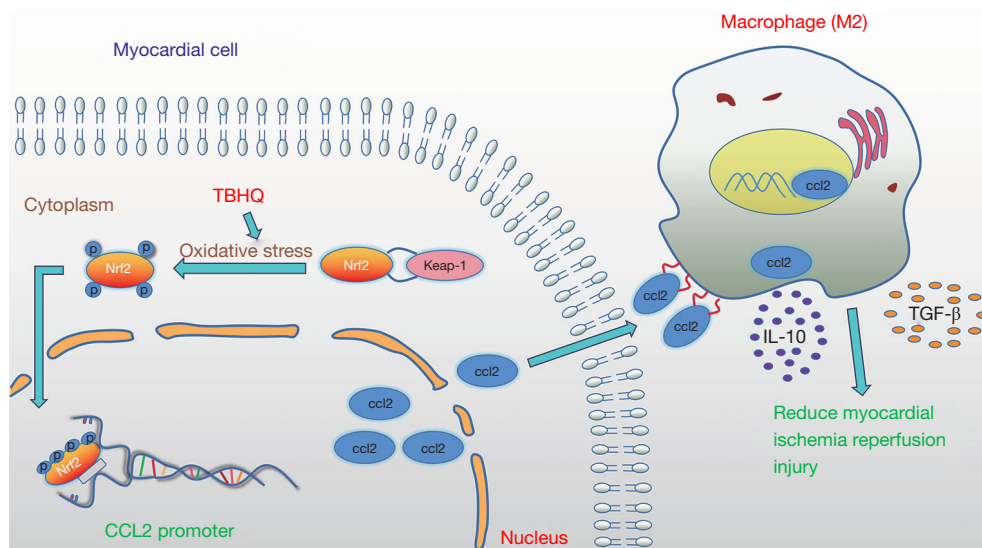


Figure 8 A graphic description of the possible mechanism by which TBHQ protects against ischemia-reperfusion injury. TBHQ activates Nrf2 into P-Nrf2, which then promotes the secretion of Ccl2 and the subsequent recruitment of M2 type macrophages to release inflammatory factors IL-10 and TGF- β 1. This results in reduced MIRI. TBHQ, tertiary butylhydroquinone; Nrf2, nuclear factor erythroid 2-related factor 2; P-Nrf2, phosphorylated Nrf2; Ccl2, C-C motif chemokine ligand 2; IL, interleukin; TGF, tumor growth factor; MIRI, myocardial ischemia-reperfusion injury.

the activation of macrophages and downregulate the release of pro-inflammatory cytokines, and nitrogen substances (43). TGF- β 1 can induce a M2-like phenotype in macrophages, which are characterized by the upregulation of the anti-inflammatory cytokine IL-10 and the downregulation of the pro-inflammatory cytokines TNF- α and IL-12. In the healthy intestine, the immunosuppressive M2 macrophage phenotype is superior to the M1 phenotype; however, in the inflamed intestinal mucosa, resident macrophages show an inflammatory M1 phenotype. The intestinal tissue is the body's largest mucosal immune site. Innate immunity, as the first line of defense, is essential for maintaining the balance of the intestinal immune microenvironment. The synergistic effect of Ccl2 and the CXC motif12 chemokine (CXCL12) determines the polarization of IL-10 + macrophages in a CCR2-dependent manner (44). In addition, the shift in the balance between M1 and M2 macrophages facilitates earlier and increased numbers of M2 macrophage infiltration, which may be a potential target for the treatment of MIRI.

There were several limitations to this study. First, it remains undetermined which subtype of macrophages, M2a, M2b, M2C, or M2d, were recruited by Ccl2. Second, the precise mechanisms by which the recruited macrophages

are polarized from M1 type to M2 type remains to be elucidated. Future studies should also investigate the dose relationship between TBHQ and the M1 to M2 transition.

This study predicted the binding of Nrf2 to the promoter region of Ccl2 using the Jasp database and examined the relationship between Nrf2 and Ccl2. Furthermore, the association between Nrf2 activation and macrophage infiltration and migration was investigated. The results demonstrated that in the early stages of ischemia-reperfusion and after being stimulated by oxidative stress, TBHQ causes the activation of Nrf2 into P-Nrf2, which in turn promotes the transcription of Ccl2. This results in the recruitment of M2 macrophages and the release of anti-inflammatory factors including TGF- β 1 and IL-10.

Acknowledgments

Funding: This work was supported by the National Natural Science Foundation of China (81770266), Clinical Medical Research Center of Cardiothoracic Diseases in Nantong (HS2019001), Innovation Team of Cardiothoracic Disease in Affiliated Hospital of Nantong University (TECT-A04), and Nantong Key Laboratory of Translational Medicine of

Cardiothoracic Diseases.

Footnote

Reporting Checklist: The authors have completed the ARRIVE reporting checklist. Available at <https://dx.doi.org/10.21037/atm-21-2947>

Data Sharing Statement: Available at <https://dx.doi.org/10.21037/atm-21-2947>

Conflicts of Interest: All authors have completed the ICMJE uniform disclosure form (available at <https://dx.doi.org/10.21037/atm-21-2947>). The authors have no conflicts of interest to declare.

Ethical Statement: The authors are accountable for all aspects of the work in ensuring that questions related to the accuracy or integrity of any part of the work are appropriate investigated and resolved. All animal experiments were approved by the Medical Ethics Committee of Nantong University and conducted in accordance with the guidance of the Experimental Institute of Nantong University. The study was approved by the ethics board of the Affiliated Hospital of Nantong University (No. S20200314-012).

Open Access Statement: This is an Open Access article distributed in accordance with the Creative Commons Attribution-NonCommercial-NoDerivs 4.0 International License (CC BY-NC-ND 4.0), which permits the non-commercial replication and distribution of the article with the strict proviso that no changes or edits are made and the original work is properly cited (including links to both the formal publication through the relevant DOI and the license). See: <https://creativecommons.org/licenses/by-nc-nd/4.0/>.

References

- Mokhtari-Zaer A, Marefati N, Atkin SL, et al. The protective role of curcumin in myocardial ischemia-reperfusion injury. *J Cell Physiol* 2018;234:214-22.
- Xu Y, Guo W, Zeng D, et al. Inhibiting miR-205 Alleviates Cardiac Ischemia/Reperfusion Injury by Regulating Oxidative Stress, Mitochondrial Function, and Apoptosis. *Oxid Med Cell Longev* 2021;2021:9986506.
- Jiang X, Wu D, Jiang Z, et al. Protective Effect of Nicorandil on Cardiac Microvascular Injury: Role of Mitochondrial Integrity. *Oxid Med Cell Longev* 2021;2021:4665632.
- Ye J, Wang R, Wang M, et al. Hydroxysafflor Yellow A Ameliorates Myocardial Ischemia/Reperfusion Injury by Suppressing Calcium Overload and Apoptosis. *Oxid Med Cell Longev* 2021;2021:6643615.
- Cadenas S. ROS and redox signaling in myocardial ischemia-reperfusion injury and cardioprotection. *Free Radic Biol Med* 2018;117:76-89.
- Meng X, Zhang C, Guo Y, et al. TBHQ Attenuates Neurotoxicity Induced by Methamphetamine in the VTA through the Nrf2/HO-1 and PI3K/AKT Signaling Pathways. *Oxid Med Cell Longev* 2020;2020:8787156.
- Silva-Palacios A, Colín-González AL, López-Cervantes SP, et al. Tert-butylhydroquinone pre-conditioning exerts dual effects in old female rats exposed to 3-nitropropionic acid. *Redox Biol* 2017;12:610-24.
- Ciccarelli O, Colson A, De Saeger C, et al. Tumoral response and tumoral phenotypic changes in a rat model of diethylnitrosamine-induced hepatocellular carcinoma after salirasib and sorafenib administration. *Onco Targets Ther* 2018;11:7143-53.
- Soyman Z, Uzun H, Bayindir N, et al. Can ebselen prevent cisplatin-induced ovarian damage? *Arch Gynecol Obstet* 2018;297:1549-55.
- Sari E, Bakar B, Sarkarati B, et al. Effectiveness of Dimethylsulfoxide on the Survival and Volume Preservation of Autologous Fat Graft Tissue: A Preliminary Study. *Aesthet Surg J* 2016;36:NP58-67.
- Li W, Lu M, Zhang Y, et al. Puerarin attenuates the daunorubicin-induced apoptosis of H9c2 cells by activating the PI3K/Akt signaling pathway via the inhibition of Ca²⁺ influx. *Int J Mol Med* 2017;40:1889-94.
- Zou J, Zhang Y, Sun J, et al. Deoxyelephantopin Induces Reactive Oxygen Species-Mediated Apoptosis and Autophagy in Human Osteosarcoma Cells. *Cell Physiol Biochem* 2017;42:1812-21.
- Cao L, Wang H, Wang F, et al. β -induced senescent retinal pigment epithelial cells create a proinflammatory microenvironment in AMD. *Invest Ophthalmol Vis Sci* 2013;54:3738-50.
- Qian J, Jiang F, Wang B, et al. Ophiopogonin D prevents H₂O₂-induced injury in primary human umbilical vein endothelial cells. *J Ethnopharmacol* 2010;128:438-45.
- Yang QH, Yang M, Zhang LL, et al. The mechanism of miR-23a in regulating myocardial cell apoptosis through targeting FoxO3. *Eur Rev Med Pharmacol Sci* 2017;21:5789-97.
- Gan S, Su C, Ma J, et al. Translation of Tudor-SN, a novel

- terminal oligo-pyrimidine (TOP) mRNA, is regulated by the mTORC1 pathway in cardiomyocytes. *RNA Biol* 2021;18:900-13.
17. Tsai KL, Hsieh PL, Chou WC, et al. Dapagliflozin attenuates hypoxia/reoxygenation-caused cardiac dysfunction and oxidative damage through modulation of AMPK. *Cell Biosci* 2021;11:44.
 18. European Food Safety Authority (EFSA); Zancanaro G. Annual assessment of *Echinococcus multilocularis* surveillance reports submitted in 2020 in the context of Commission Delegated Regulation (EU) 2018/772. *EFSA J* 2021;19:e06382.
 19. Wang G, Jiang L, Song J, et al. Mipu1 protects H9c2 myogenic cells from hydrogen peroxide-induced apoptosis through inhibition of the expression of the death receptor Fas. *Int J Mol Sci* 2014;15:18206-20.
 20. Shi YN, Zhang XQ, Hu ZY, et al. Genistein Protects H9c2 Cardiomyocytes against Chemical Hypoxia-Induced Injury via Inhibition of Apoptosis. *Pharmacology* 2019;103:282-90.
 21. Gu M, Wang J, Wang Y, et al. MiR-147b inhibits cell viability and promotes apoptosis of rat H9c2 cardiomyocytes via down-regulating KLF13 expression. *Acta Biochim Biophys Sin (Shanghai)* 2018;50:288-97.
 22. Yao C, Li G, Qian Y, et al. Protection of Pentoxifylline against Testis Injury Induced by Intermittent Hypobaric Hypoxia. *Oxid Med Cell Longev* 2016;2016:3406802.
 23. Yu H, Chen B, Ren Q. Baicalin relieves hypoxia-aroused H9c2 cell apoptosis by activating Nrf2/HO-1-mediated HIF1 α /BNIP3 pathway. *Artif Cells Nanomed Biotechnol* 2019;47:3657-63.
 24. Li M, Ye J, Zhao G, et al. Gas6 attenuates lipopolysaccharide induced TNF α expression and apoptosis in H9C2 cells through NF κ B and MAPK inhibition via the Axl/PI3K/Akt pathway. *Int J Mol Med* 2019;44:982-94.
 25. Pang B, Shi LW, Du LJ, et al. Sheng Mai San protects H9C2 cells against hyperglycemia-induced apoptosis. *BMC Complement Altern Med* 2019;19:309.
 26. Choi JW, Lee KH, Kim SH, et al. C-reactive protein induces p53-mediated cell cycle arrest in H9c2 cardiac myocytes. *Biochem Biophys Res Commun* 2011;410:525-30.
 27. Marek-Iannucci S, Thomas A, Hou J, et al. Myocardial hypothermia increases autophagic flux, mitochondrial mass and myocardial function after ischemia-reperfusion injury. *Sci Rep* 2019;9:10001.
 28. DuSablon A, Parks J, Whitehurst K, et al. EphrinA1-Fc attenuates myocardial ischemia/reperfusion injury in mice. *PLoS One* 2017;12:e0189307.
 29. Zhang L, Yu M, Deng J, et al. Chemokine Signaling Pathway Involved in CCL2 Expression in Patients with Rheumatoid Arthritis. *Yonsei Med J* 2015;56:1134-42.
 30. Zhang Y, Wang S, Huang Y, et al. Inhibition of CYP1B1 ameliorates cardiac hypertrophy induced by uremic toxin. *Mol Med Rep* 2020;21:393-404.
 31. He F, Wu Q, Xu B, et al. Suppression of Stim1 reduced intracellular calcium concentration and attenuated hypoxia/reoxygenation induced apoptosis in H9C2 cells. *Biosci Rep* 2017;37:BSR20171249.
 32. Yang C, Wei C, Wang S, et al. Elevated CD163+/CD68+ Ratio at Tumor Invasive Front is Closely Associated with Aggressive Phenotype and Poor Prognosis in Colorectal Cancer. *Int J Biol Sci* 2019;15:984-98.
 33. Wu CY, Yang HY, Huang JL, et al. Signals and Mechanisms Regulating Monocyte and Macrophage Activation in the Pathogenesis of Juvenile Idiopathic Arthritis. *Int J Mol Sci* 2021;22:7960.
 34. Wang J, Xu L, Xiang Z, et al. Microcystin-LR ameliorates pulmonary fibrosis via modulating CD206+ M2-like macrophage polarization. *Cell Death Dis* 2020;11:136.
 35. Liu F, Qiu H, Xue M, et al. MSC-secreted TGF- β regulates lipopolysaccharide-stimulated macrophage M2-like polarization via the Akt/FoxO1 pathway. *Stem Cell Res Ther* 2019;10:345.
 36. Götze AM, Schubert C, Jung G, et al. IL10 Alters Peri-Collateral Macrophage Polarization and Hind-Limb Reperfusion in Mice after Femoral Artery Ligation. *Int J Mol Sci* 2020;21:2821.
 37. Zeng H, Wang L, Zhang J, et al. Activated PKB/GSK-3 β synergizes with PKC- δ signaling in attenuating myocardial ischemia/reperfusion injury via potentiation of NRF2 activity: Therapeutic efficacy of dihydrotanshinone-I. *Acta Pharm Sin B* 2021;11:71-88.
 38. Zhang J, Cai X, Zhang Q, et al. Hydrogen sulfide restores sevoflurane postconditioning mediated cardioprotection in diabetic rats: Role of SIRT1/Nrf2 signaling-modulated mitochondrial dysfunction and oxidative stress. *J Cell Physiol* 2021;236:5052-68.
 39. Huang HC, Nguyen T, Pickett CB. Phosphorylation of Nrf2 at Ser-40 by protein kinase C regulates antioxidant response element-mediated transcription. *J Biol Chem* 2002;277:42769-74.
 40. Villarreal-Ponce A, Tiruneh MW, Lee J, et al. Keratinocyte-Macrophage Crosstalk by the Nrf2/Ccl2/EGF Signaling Axis Orchestrates Tissue Repair. *Cell Rep*

- 2020;33:108417.
41. Sierra-Filardi E, Nieto C, Domínguez-Soto A, et al. CCL2 shapes macrophage polarization by GM-CSF and M-CSF: identification of CCL2/CCR2-dependent gene expression profile. *J Immunol* 2014;192:3858-67.
 42. Markowski P, Boehm O, Goelz L, et al. Pre-conditioning with synthetic CpG-oligonucleotides attenuates myocardial ischemia/reperfusion injury via IL-10 up-regulation. *Basic Res Cardiol* 2013;108:376.
 43. Yang D, Dai F, Yuan M, et al. Role of Transforming Growth Factor- β 1 in Regulating Fetal-Maternal Immune Tolerance in Normal and Pathological Pregnancy. *Front Immunol* 2021;12:689181.
 44. Giri J, Das R, Nysten E, et al. CCL2 and CXCL12 Derived from Mesenchymal Stromal Cells Cooperatively Polarize IL-10+ Tissue Macrophages to Mitigate Gut Injury. *Cell Rep* 2020;30:1923-1934.e4.

(English Language Editors: J. Teoh and J. Gray)

Cite this article as: Huang Z, Li X, Zhou T, Jiang Y, Shi JH. Phosphorylated nuclear factor erythroid 2-related factor 2 promotes the secretion of C-C motif chemokine ligand 2 and the recruitment of M2 macrophages. *Ann Transl Med* 2021;9(23):1719. doi: 10.21037/atm-21-2947